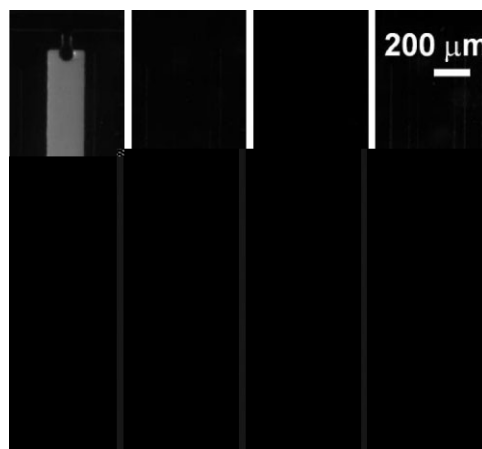


Constructing the Phase Diagram of an Aqueous Solution of Poly(*N*-isopropyl acrylamide) by Controlled Microevaporation in a Nanoliter Microchamber

Xuechang Zhou, Junfang Li, Chi Wu, Bo Zheng*

This paper describes a poly(dimethylsiloxane) (PDMS)-based microfluidic platform for constructing the phase diagram of poly(*N*-isopropyl acrylamide) (PNIPAM) in aqueous solution. The PNIPAM solution was delivered into a nanoliter chamber through the main microchannel. An osmotic pressure difference was established between the chamber and the control microchannel by flowing a high-concentration salt solution in the control microchannel. Controlled evaporation of water resulted in increasing concentration of PNIPAM. A phase diagram of PNIPAM was built by measuring the cloud points at different concentrations, with a minimum point at ≈ 40 wt.-%. The microfluidic platform has the advantages of low sample consumption and rapid heat exchange rates, and allows studying viscous polymer solution.



Introduction

This paper describes a simple poly(dimethylsiloxane) (PDMS)-based microfluidic platform for constructing the phase diagram of poly(*N*-isopropyl acrylamide) (PNIPAM) in aqueous solution in a nanoliter microchamber. Different from small molecules, polymer phase diagrams depend on the chain length. The chain lengths of synthetic polymers

are normally broadly distributed. To our knowledge, there is a lack of phase diagrams for most polymers, which is mainly due to two reasons: 1) lack of sufficient amount of narrowly distributed polymer samples with different chain lengths; and 2) an extremely long time required for a viscous polymer solution to reach its phase equilibrium, especially when the concentration is high. Phase transition of solutions of thermosensitive polymers, such as PNIPAM, which exhibits a lower critical solution temperature (LCST), has been widely investigated by various experimental techniques, including IR spectroscopy,^[1] ¹H NMR spectroscopy,^[2] viscometry,^[3,4] fluorescence,^[5] turbidimetry,^[6] light scattering,^[7] and calorimetry.^[8] These studies of the phase transition behavior were generally carried out in conventional reaction vessels with volume of 1 mL or more. There are two associated issues as aforementioned, i.e., the lack of sufficient amount of narrowly distributed polymer

X. Zhou, C. Wu, B. Zheng

Department of Chemistry, The Chinese University of Hong Kong, Shatin, Hong Kong

Fax: +852-2603 5057; E-mail: bozheng@cuhk.edu.hk

J. Li

National Laboratory for Physical Sciences at Microscale, Department of Chemical Physics, University of Science and Technology of China, Hefei, Anhui 230026, China

sample and long phase equilibrium time. As a result, systematic experimental investigations on the phase diagram of PNIPAM/water solution have not been accomplished, and the concentration and molecular weight dependence of the cloud point of PNIPAM aqueous solutions are still controversial.^[8–12]

The microfluidics platform, with the advantages of small volume consumption, rapid heat exchange rate and high-throughput capability has been applied to study the phase behavior and other properties of macromolecules.^[13–16] Cremer and coworkers developed a microfluidic device that allowed rapid measurements of the phase separation temperatures of thermosensitive polymer solution stored in glass capillaries.^[12,13,17] However, this method required advance preparation of each concentration of the polymer solution to be measured, and it was not feasible for high concentration polymer solution which was too viscous for sample loading. On the other hand, the water permeability of PDMS elastomer^[18] has been exploited to vary the concentration of solutions in the PDMS-based microfluidic device. For example, Leng et al. developed a PDMS micro-evaporator to concentrate ionic and colloidal solutions,^[14] and Lau et al. developed a dynamic osmotic bath for screening conditions of protein crystallization.^[16] A “phase chip” was recently designed for studying the phase diagram of various aqueous solutions.^[15] These methods demonstrated the feasibility of preparing high concentration with an initial dilute solution by using microfluidic devices. However, all these works utilized multilayer PDMS microfluidic device, which are complicated to fabricate and operate.

Here, we developed a single-layer, microchamber-based microfluidic device to study the phase separation behavior of PNIPAM in aqueous solution. By confining the polymer solution in a PDMS microchamber, we were able to concentrate the solution by more than three times and study the phase transition. Comparing to the previous microfluidic devices mentioned above, not only the fabrication and operation are significantly easier, but also the single-layer microchannel facilitates better observation of the phase transition of polymer solutions, e.g., the cloud point.

Experimental Part

The PNIPAM polymer was synthesized via free radical polymerization^[7] and was fractionated using a mixture of acetone/hexane at room temperature. The fractionated PNIPAM with a weight-averaged molecular weight (\overline{M}_w , characterized by laser light scattering) of $3.9 \cdot 10^5 \text{ g} \cdot \text{mol}^{-1}$ and the polydispersity index (PDI, determined by gel permeation chromatography) of 1.10 was chosen for the present study. Two concentrations of the PNIPAM solution in deionized water, 18.2 wt.-% and 4.9 wt.-%, were prepared and used in our experiments.

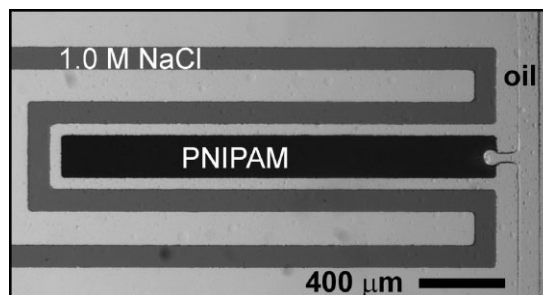


Figure 1. Bright-field micrograph of the microchamber filled with an 18.2 wt.-% PNIPAM aqueous solution at 35 °C (above the phase separation temperature), the main channel filled with paraffin oil and the control channel filled with 1.0 M NaCl aqueous solution. 0.5 M $\text{Fe}(\text{SCN})_x^{3-x}$ aqueous solution was added to the NaCl solution for better observation.

The microfluidic device was fabricated by irreversibly binding a PDMS slab onto a flat glass slide. The glass slide was pre-coated with a thin layer of PDMS. The PDMS slab containing the feature of the microchamber and the microchannels was fabricated by soft lithography.^[19] The microfluidic device contained a microchamber (width 200 μm · length 2 000 μm · height 100 μm), a main channel (width 100 μm · height 100 μm), and a control channel (width 100 μm · height 100 μm). The main channel was connected with the microchamber while separated from the control channel (Figure 1).

The PNIPAM aqueous solution was delivered into the microchamber following a previously reported procedure.^[20] Briefly, the PDMS device was pre-degassed in a vacuum chamber for 20 minutes. 1–2 μL of PNIPAM aqueous solution was preloaded into a segment of Teflon tubing, and the Teflon tubing was inserted into the inlet of the main channel. The outlet of the main channel was also blocked, and vacuum was generated in the main channel and in the microchamber as the air was gradually absorbed into PDMS. As a result, the PNIPAM solution was aspirated into the main channel and the microchamber. After the completion of the filling of PNPAM aqueous solution (18.2 wt.-% or 4.9 wt.-%), paraffin oil was introduced to purge the PNIPAM aqueous solution out of the main channel and confine the PNIPAM solution in the microchamber. To concentrate the PNIPAM solution, 1.0 M of NaCl aqueous solution was flowed continuously in the control channel at a flow rate of 0.5 $\mu\text{L} \cdot \text{min}^{-1}$ (Figure 1).

Cloud point measurements were carried out when a certain concentration of PNIPAM was reached during the concentrating process. The microfluidic device was placed on a programmable Pelt-Plate Intelligent HOT/COLD Plate (Sable Systems International, PELT-5), which was heated or cooled at a rate of 0.5 °C · min⁻¹. The temperature of the microchannel and the microchamber was recorded by a thermocouple meter (Sable Systems International, TC-2000) which was coupled to the microfluidic device. The phase separation behavior was monitored using a CCD camera (Diagnostic Instruments, SPOT Insight) coupled with a 3× telecentric lens (Daheng) during the heating or cooling process. Series of images were recorded at a speed of 1 frame every 15 sec. A home-built LED lamp was used as the light source. The intensity of the scattered light from the PNIPAM

solution was measured by ImageJ (NIH). The cloud point was determined as the temperature at which the initial increase of the scattered intensity appeared from the clouding curve during the heating process.^[6] We also constructed the clearing curve by measuring the scattered intensity during the cooling process. After the completion of the heating and cooling processes at each concentration, the microfluidic device was cooled down to 15 °C.

Results and Discussion

A series of PNIPAM aqueous solution with increasing concentration was generated by controlled microevaporation of water in the PDMS microchamber. It has been shown that small neutral molecules such as water can permeate through PDMS relatively easily,^[14,16,18,21] while such permeation is non-detectable for ions, such as Na⁺ and Cl⁻, and for macromolecules such as poly(ethylene glycol) and proteins.^[15] In the current microfluidic device, there existed an osmotic pressure difference between the PNIPAM solution and the NaCl solution. Water gradually permeated through PDMS from the PNIPAM solution to the NaCl solution, thereby increasing the concentration of PNIPAM. By measuring the volume change of the PNIPAM solution, we were able to determine the concentration of PNIPAM. In addition, the rate of water permeation can be both accelerated and decelerated using different salt concentrations in the control channel.^[15] It is also possible to fine-tune the salt concentration to stop water permeation,^[22] so that the polymer solution will remain at a defined concentration for long-term study. In our experiment, 1.0 M NaCl aqueous solution was continuously flowed in the control channel at a flow rate of 0.5 $\mu\text{L} \cdot \text{min}^{-1}$. The change of the concentration of PNIPAM in the microchamber is shown in Figure 2. With an initial 40 nL volume of PNIPAM aqueous solution of a given starting concentration (4.9 wt.-% and 18.2 wt.-%, respectively), we were able to generate a series of PNIPAM aqueous solutions *in situ* with increasing concentrations, covering a wide range from 5 wt.-% to 60 wt.-%.

As an LCST type polymer, PNIPAM aqueous solution is homogeneous and transparent at temperature lower than LCST, and undergoes a phase separation upon heating beyond the LCST. Such phase separation causes the increase of the scattered light intensity. Figure 3 shows a typical clouding and clearing curve of PNIPAM aqueous solution at the concentration of 15.2 wt.-%. From the clouding curve, the cloud point was determined at 30.0 °C. Due to the small scale of the microchamber (40 nL), the thermal equilibrium between the hotplate and the PNIPAM solution was rapidly established at each temperature point. Remarkably, at each measured concentration we observed that the clouding and clearing curves were well-overlapped, indicating a reversible phase

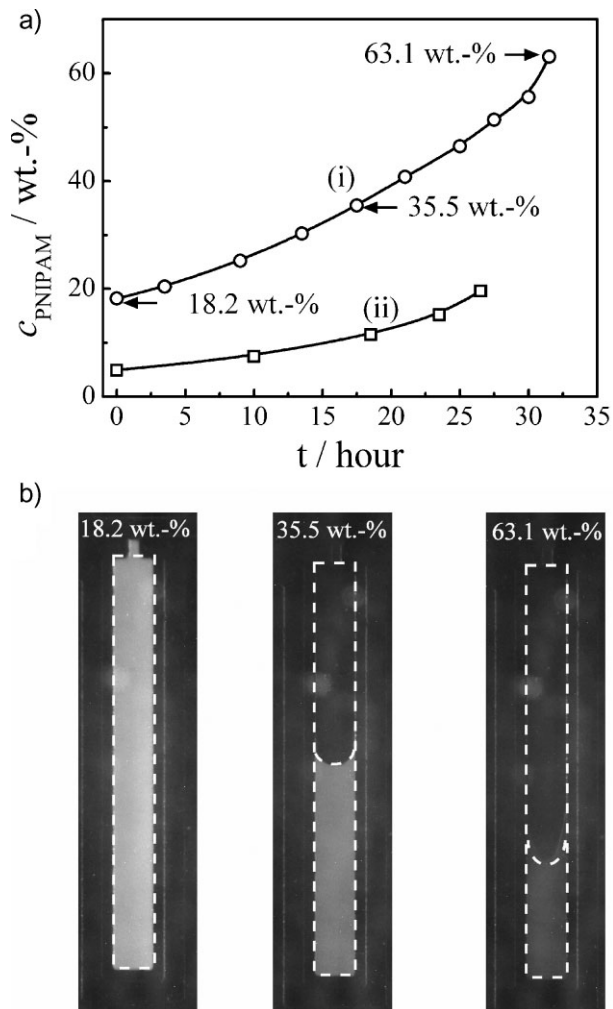


Figure 2. (a) Time dependence of the concentrations of the PNIPAM aqueous solution in the 40 nL microchamber, with the initial concentrations of 18.2 wt.-% (i) and 4.9 wt.-% (ii), respectively. 1.0 M NaCl aqueous solution was flowed in the control channel at the flow rate of 0.5 $\mu\text{L} \cdot \text{min}^{-1}$; (b) CCD images of PNIPAM aqueous solutions at the indicated concentrations: 18.2, 35.5, and 63.1 wt.-%, respectively. The white dashed line outlines the microchamber (width 200 μm and length 2 mm) as well as the interface between the PNIPAM solution and the paraffin oil.

transition of the PNIPAM aqueous solution. The rapid thermal equilibrium in the microchamber enabled us to obtain the clouding and clearing curves within a short duration of measurement (≈ 10 min). No noticeable change of the solution volume occurred in such a short duration, as indicated by the controlled microevaporation process (Figure 2); therefore, it is a valid assumption that the concentration remained constant during each heating and cooling processes.

The cloud points of a series of concentrations ranging from 5 wt.-% to 60 wt.-% were measured to build the phase diagram of PNIPAM aqueous solution (Figure 4). Our

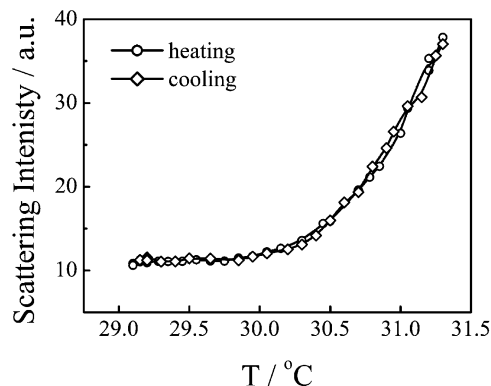


Figure 3. Clouding and clearing curves of the PNIPAM aqueous solution with the concentration of 15.2 wt.-% in the microchamber.

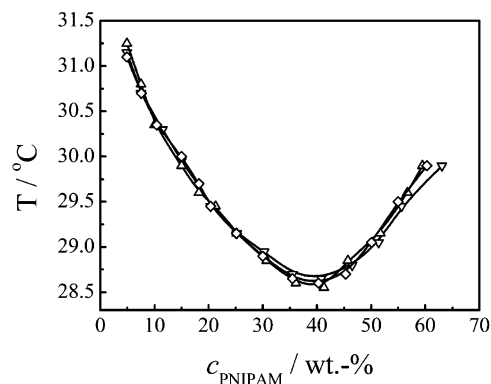


Figure 4. Phase diagram showing the concentration dependence of the phase separation temperatures of PNIPAM aqueous solution. The three curves are from three parallel measurements.

measurement showed that the phase separation temperatures decreased as the concentration increased in the low concentration region ($c_{\text{PNIPAM}} < 40$ wt.-%) (Figure 4). Most of the previous studies about the concentration effect on the phase separation temperature of PNIPAM were limited to the concentration lower than 40%,^[6,12] and our observation showed good agreement. On the other hand, in the high concentration region ($c_{\text{PNIPAM}} > 40$ wt.-%), the phase separation temperature increased as the concentration increased, with a minimum point of the phase separation temperatures at the concentration around 40 wt.-%. This observation was consistent with the results reported by Afroze et al.^[23] and by Van Durme et al.^[11]

Conclusion

In conclusion, a microfluidic method was developed to construct the phase diagram of PNIPAM aqueous solution.

This method has the advantages of simple execution, low sample consumption, rapid heat exchange, and capability of studying high concentration solution. We successfully concentrated the PNIPAM solution to higher than 60 wt.-% by controlled microevaporation, while being still able to characterize the phase transition in a short duration. The ultrasmall reagent consumption (1 to 2 μL) is important to the study of narrowly distributed polymer sample, which is usually difficult to obtain and the amount is limited. We believe that the microfluidic method is capable of a systematic investigation to ultimately settle the dispute on the effects of concentration and molecular weight on the phase separation temperatures of the PNIPAM aqueous solution.^[9,10,12,24] The throughput of the device can be enhanced by improving the following factors: (1) the number of microchambers on the device; (2) the rate of water permeation, which depends on the salt concentration and the PDMS wall thickness between the control channel and the microchamber; (3) the view area of the optical detection setup. Due to the incompatibility of PDMS with many organic solvents,^[25] the current PDMS microfluidic device can not be applied to organic solutions. We envision that this issue can be solved by using fluorinated elastomers as the material of the microfluidic device.^[26,27] More work is underway to extend the application of this method to other macromolecule solutions, such as copolymers, polymer mixtures, and proteins.

Acknowledgements: This research is supported by the *Chinese University of Hong Kong* and the *Research Grants Council of Hong Kong* (Project 404406) to B. Z.

Received: April 16, 2008; Revised: May 17, 2008; Accepted: May 19, 2008; DOI: 10.1002/marc.200800229

Keywords: microfluidics; osmotic pressure; phase diagram; polysiloxanes; water-soluble polymers

- [1] J. S. Scarpa, D. D. Mueller, I. M. Klotz, *J. Am. Chem. Soc.* **1967**, *89*, 6024.
- [2] H. Ohta, I. Ando, S. Fujishige, K. Kubota, *J. Polym. Sci., Part B: Polym. Phys.* **1991**, *29*, 963.
- [3] K. Kubota, S. Fujishige, I. Ando, *Polym. J.* **1990**, *22*, 15.
- [4] H. Yang, X. H. Yan, R. S. Cheng, *J. Polym. Sci., Part B: Polym. Phys.* **2000**, *38*, 1188.
- [5] F. M. Winnik, *Macromolecules* **1990**, *23*, 233.
- [6] C. Boutris, E. G. Chatzi, C. Kiparissides, *Polymer* **1997**, *38*, 2567.
- [7] C. Wu, S. Q. Zhou, *Macromolecules* **1995**, *28*, 8381.
- [8] H. G. Schild, D. A. Tirrell, *J. Phys. Chem.* **1990**, *94*, 4352.
- [9] S. Fujishige, K. Kubota, I. Ando, *J. Phys. Chem.* **1989**, *93*, 3311.
- [10] Z. Tong, F. Zeng, X. Zheng, T. Sato, *Macromolecules* **1999**, *32*, 4488.
- [11] K. Van Durme, G. Van Assche, B. Van Mele, *Macromolecules* **2004**, *37*, 9596.

- [12] S. Furyk, Y. Zhang, D. Ortiz-Acosta, P. S. Cremer, D. E. Bergbreiter, *J. Polym. Sci., Part A: Polym. Chem.* **2006**, *44*, 1492.
- [13] H. B. Mao, C. M. Li, Y. J. Zhang, D. E. Bergbreiter, P. S. Cremer, *J. Am. Chem. Soc.* **2003**, *125*, 2850.
- [14] J. Leng, B. Lonetti, P. Tabeling, M. Joanicot, A. Ajdari, *Phys. Rev. Lett.* **2006**, *96*.
- [15] J. U. Shim, G. Cristobal, D. R. Link, T. Thorsen, Y. W. Jia, K. Piattelli, S. Fraden, *J. Am. Chem. Soc.* **2007**, *129*, 8825.
- [16] B. T. C. Lau, C. A. Baitz, X. P. Dong, C. L. Hansen, *J. Am. Chem. Soc.* **2007**, *129*, 454.
- [17] H. Mao, C. Li, Y. Zhang, S. Furyk, P. S. Cremer, D. E. Bergbreiter, *Macromolecules* **2004**, *37*, 1031.
- [18] G. C. Randall, P. S. Doyle, *Proc. Natl. Acad. Sci. USA* **2005**, *102*, 10813.
- [19] D. C. Duffy, J. C. McDonald, O. J. A. Schueller, G. M. Whitesides, *Anal. Chem.* **1998**, *70*, 4974.
- [20] X. Zhou, L. Lau, W. W. L. Lam, S. W. N. Au, B. Zheng, *Anal. Chem.* **2007**, *79*, 4924.
- [21] J. M. Watson, M. G. Baron, *J. Membr. Sci.* **1995**, *106*, 259.
- [22] B. Zheng, L. S. Roach, R. F. Ismagilov, *J. Am. Chem. Soc.* **2003**, *125*, 11170.
- [23] F. Afroze, E. Nies, H. Berghmans, *J. Mol. Struct.* **2000**, *554*, 55.
- [24] F. M. Winnik, *Polymer* **1990**, *31*, 2125.
- [25] J. N. Lee, C. Park, G. M. Whitesides, *Anal. Chem.* **2003**, *75*, 6544.
- [26] J. P. Rolland, R. M. Van Dam, D. A. Schorzman, S. R. Quake, J. M. DeSimone, *J. Am. Chem. Soc.* **2004**, *126*, 2322.
- [27] Y. Y. Huang, P. Castrataro, C. C. Lee, S. R. Quake, *Lab Chip* **2007**, *7*, 24.